

The analysis of nuclear tracks with confocal microscopy and image restoration

Filip Rooms⁽¹⁾ Wilfried Philips⁽¹⁾
Geert Meesen⁽²⁾ Patric Van Oostveldt⁽³⁾
Ghent University

⁽¹⁾TELIN, Sint-Pietersnieuwstraat 41, B9000 Ghent

⁽²⁾RADIATION AND ENVIRONMENTAL PHYSICS, Proeftuinstraat 86, B9000 Ghent

⁽³⁾MOLECULAR BIOCHEMISTRY, Coupure links 653, B9000 Ghent
BELGIUM

Filip.Rooms@rug.ac.be <http://telin.rug.ac.be/frooms/>

Abstract: - To measure radiation damage of particles with high energy and charge in space, radiosensitive plastics are used, in which particles leave damage tracks where they pass. These tracks are then etched, after which they have a typical cone shape. The geometrical parameters of these cones give information about energy and charge of the particles. To measure these parameters, the tracks are recorded in three dimensions with a confocal microscope, which is a special kind of microscope that can make threedimensional images of an object. To reduce blur in the recorded images of the tracks, image restoration is used. But with blur removal, the risk is that noise is amplified. Three techniques that handle this problem are compared: the wienerfilter, iterative constrained Tikhonov-Miller and Richardson-Lucy. The first two methods increase sharpness of the image, but also let noise as data. Richardson-Lucy is the best method, but has a very slow convergence rate. After the image is restored, the geometrical parameters of the damage cones are extracted from the image by fitting cone models to the image.

Key-Words: - Confocal microscopy, nuclear tracks, space environment, image restoration.

1 Introduction

In this paper, a method is described to analyse heavy ionising radiation. This method was used in an experiment, performed at Ghent University in collaboration with ESA (European Space Agency). The objective of the experiment is to study the effect of radiation in space on biological cells to obtain a better insight in the risk of prolonged exposure of astronauts to radiation in space. The following topics will be discussed.

We will start with a discussion of the different kinds of radiation in space to which the astronauts are exposed during space missions.

After that, we will explain the principles of a special kind of passive detectors, so called Solid State Nuclear Track Detectors (SSNTD) [5,9,14,15]. These detectors are in fact pieces of plastic, in which the particle leaves a damage trail by breaking the polymere chains as it passes through the plastic. This damage is not visible with conven-

tional equipment, but can be enlarged by chemical etching. These etch pits then are visible as small cones in a microscope.

To study the exact threedimensional form of the etch pits, a special kind of microscope was used, i.e., a Confocal Scanning Laser Microscope (CSLM) [6,10]. This kind of microscope allows visualising threedimensional volumes by imaging thin slices through the specimen.

The next step is the optimisation of the image quality by applying deconvolution. In this part, some different algorithms will be discussed with advantages and disadvantages.

Finally, a cone fitting algorithm will be applied to the image in order to determine the geometrical parameters of the track cones, which are related to the energy and charge of the detected particles.

2 Radiation in space.

In the discussed experiment, radiation is not electromagnetic radiation, but consists of heavy ionizing particles (HZE: particles with a high atom number (Z) and a high energy (E)).

Radiation in space [2, 3, 11], can be classified in three different categories, according to its origin.

A first class of radiation in space is trapped radiation. These are particles from the solar wind, trapped in the earth magnetic field in the so-called Van Allen radiation belts. This kind of radiation is important in space missions which fly in low earth orbits (LEO). The region where the radiation has its highest intensity is the South Atlantic Anomaly. This is a place above the Atlantic Ocean where the radiation belts come much closer to the planet surface than anywhere else due to a displacement of the earth magnetic dipole with respect to the planet surface. Astronauts in LEO's get most of their radiation exposure when they pass through the South Atlantic Anomaly.

A second kind of radiation comes from Solar Particle Events (SPE). These SPE's are violent eruptions on the Sun, which emit large numbers of particles with extremely high energies. These particles can reach the neighborhood of the Earth after a couple of days. These solar storms cause moments of very high radiation intensity. These eruptions of radiation are extremely dangerous for astronauts and exposure is always to be avoided. Some eruptions can cause even lethal radiation levels in the neighborhood of the earth.

The last class is the Galactic Cosmic Radiation GCR. This is radiation from outside the solar system, caused by for example a supernova explosion (this is an explosion that occurs when a certain type of star dies). This kind of radiation consists of particles with very high energies and can almost not be shielded. Fortunately, the rate of this kind of radiation is very low.

3 Detectors and their analysis with CSLM

The detectors that are used, are in fact small pieces of a radiation sensitive plastic, of which

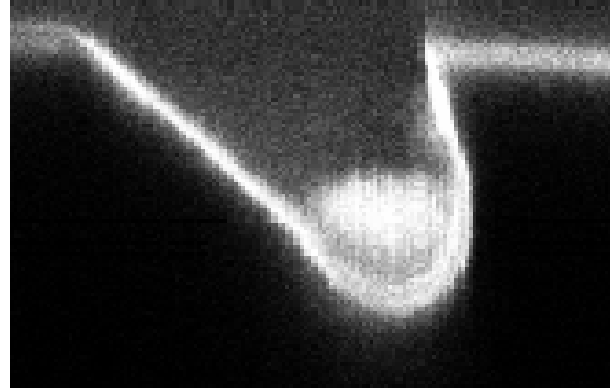


Figure 1: Etch profile of a track in the z -direction. This profile is related to the mass and the energy of the incident particle.

the polymere structure is damaged when exposed to heavy ionizing radiation. This exposed detector is then put in an etchant (in this case NaOH). The undamaged surface is dissolved at a certain rate. Along the path of the particle in the plastic, the polymere chains are damaged and the broken polymere ends caused this way are much more chemically reactive. Therefore, the etch rate along the particle tracks is much bigger. This causes a cone shaped etch pit for particles with a high linear energy transfer and very high energies. This is true for particles in space. The geometrical parameters are directly related to charge and energy of the particle which caused the damage track.

4 Imaging the detectors

After the etching process, the detectors are observed with a confocal microscope [6, 10]. This is a special kind of microscope, which allows imaging of an object point by point. This is done by illuminating the object through the objective lens. A diaphragm in front of the detector eliminates light from points that are not in focus. So a single point is imaged by this system. A scanning mechanism then measures point by point slices at different depths in a specimen. Moving the focus allows imaging slices at different depths in the specimen, thus allowing threedimensional imaging of an object. From this recording, quantitative measurements can be done.

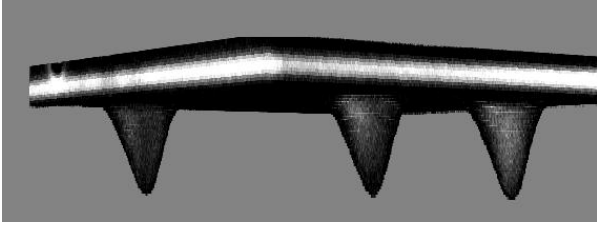


Figure 2: Threedimensional rendering of nuclear tracks from confocal image. The tracks are caused by Li-particles.

In our case, we want to measure the exact geometry of particle tracks, as seen in Figure 1. In our experiment, the etch profiles will be cone-shaped, corresponding with particles with high linear energy transfer (in contrast with the track shown in 1. So in succeeding slices through the image, we can see ellipses.

This method allowed for the first time to visualize nuclear tracks with much better precision and without damaging the original detectors. This allows analysing the detectors again in the future.

5 Image optimisation by image restoration

Optics are always limited [12], and the image formation process is determined by diffraction. An illuminated object will form a diffraction pattern because every point is a source of secondary waves, according to the Huygens principle. This diffraction pattern is proportional to the Fourier spectrum of the original object. This Fourier spectrum consists of a central peak for the DC component which can be found in the direction of the optical axis of the objective. The higher the order of the diffraction maxima, the higher the corresponding spatial frequencies are and the further away they form from the optical axis. So there is a limit to the spatial frequency which is still intercepted by the objective lens. This is a limiting factor to the resolution of the microscope. If we consider imaging a mathematical point with our microscope, the image won't be a point but a distribution of light in three dimensions. This light distribution is called the Point Spread Function (PSF).

In the observed image, points which are close to each other will be imaged as blots which can not be separated anymore. But when we know the exact shape of the PSF, certain algorithms can restore the image contents [1, 7, 8, 16–19]. A first set of algorithms performs a least-square fitting of the data to a model convolved with the PSF:

$$L(g, f) = \|g - h * f\|^2$$

with g the observed data, f the model for the solution and h the PSF. Without additional terms, this method is called the Jansson-Van Cittert algorithm. When an extra penalty term and a non-negativity constraint are added, this method is called Tikhonov-Miller restoration. The functional $\Psi(g, f)$ is given by:

$$\Psi(g, f) = \|g - h * f\|^2 + \lambda \|Cf\|^2$$

with λ the regularisation parameter and C a high-pass filter, so the second term is a measure for the energy of the high frequencies of an image. The minimisation can be done by using conjugate gradients. A variant of this method is the Carrington algorithm, which is mathematically more robust. By penalising high frequencies, the solution will be smooth. The advantage is that artifacts and noise will be penalised. The disadvantage however is that sharp edges are also penalised.

The last considered method is the *Expectation Maximisation* algorithm, also known in astronomy as the *Richardson-Lucy algorithm*. This method is based on maximising the probability $p(f | g)$ (i.e., the probability that when an image g is observed, that the original image before degradation was f) is maximal. This is calculated from $p(g | f)$, i.e., the probability that when an object f is imaged, that g will be observed. These probabilities are related by Bayes' rule:

$$p(f | g) = \frac{p(g | f) p(f)}{p(g)}$$

The denominator is just a normalisation factor and is independent of f . Easier to minimise the negative logarithm of the expression, i.e., minimising $\Psi(g, f)$.

$$\Psi(g, f) = -\ln p(g | f) - \ln p(f) = L(g, f) + P(f)$$

with $L(g, f)$ the likelihood function and $P(g, f)$ the penalty function. For gaussian noise, we find following expression for $L(g, f) = \|g - h * f\|^2$ which gives us again a least square problem. But for confocal images, it is better to consider poisson noise, which gives us another expression. One of the advantages in this approach is that no negative solutions can be found in this method, which would be meaningless anyway (negative solutions are allowed by the least square method). In fact, this general framework also includes the previous described methods by considering gaussian noise. But it is better to use poisson noise in case of confocal microscopy. In that case, we find the following functional:

$$\begin{aligned} p(g | f) &= e^{-f} f^{-g} / g! \\ \implies L(g, f) &= f + g \ln(f) - \ln(g!) \end{aligned}$$

This method gives the best results for restoration of confocal images, because the image formation process inherently involves poisson noise. It also is the best criterion when the result has to be non-negative (like in images). When this likelihood function is minimised with respect to f , one can derive the *Expectation Maximization* algorithm, equivalent to the Richardson-Lucy algorithm in astronomy. The iteration formula is given by

$$f_{k+1}(n) = f_k(n) \sum_i \left[\frac{h(i-n)}{\sum_j h(i-j) f_k(j)} \right] g(i)$$

In Figure 3, we give a comparison of the performance of the different algorithms. Here one can see that the wienerfilter gives some artifacts due to gibbs-oscillations. The Tikhonov-Miller restoration (ICTM) is already better, but also introduces some artefacts. For example, the edge of the track is smooth, as can be guessed from the original image. But after restoration, the edge of the track has a rough appearance. This is due to fitting of the noise in the solution. Then, the best is the Richardson-Lucy restoration. This method introduces least artefacts, but converges really slowly. After 20 iterations, the edge is far from sharp. It also takes more time per iteration to compute Richardson-Lucy than the other algorithms.

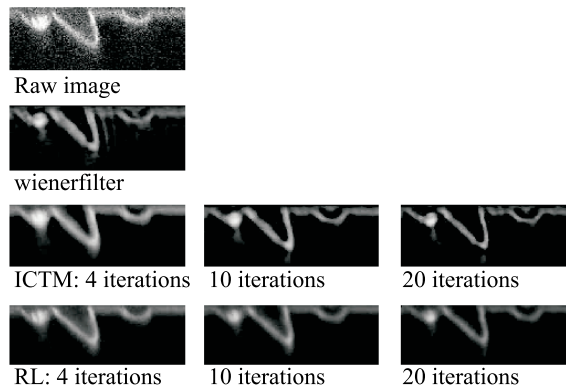


Figure 3: Comparison of the different restoration algorithms

6 Cone fitting to the restored images

After restoration of the confocal images, the recorded images can be analysed. Like was said before, the etch pits can be approximated by a cone shape. This approximation doesn't hold when tracks of particles with low energies or over-etched tracks are considered, but in our case, it can be done.

In order to fit a cone, we considered fitting of an ellipse in each section of the image [13], [4]. This procedure also gives a starting point for fitting of shapes different from a cone. Fitting of an ellipse is a difficult mathematical problem, so we did a simplification of the problem by not fitting an ellipse, but fitting a general cone section. But when there are enough data points that are on an ellipse (like in our case), the solution will be an ellipse.

We begin with the general quadratic equation of a cone section:

$$x^2 + a y^2 + b xy + c x + d y + e = 0.$$

We minimize the following expression:

$$D_s = \sum_{i=1}^N (x_i^2 + a y_i^2 + b x_i y_i + c x_i + d y_i + e)^2$$

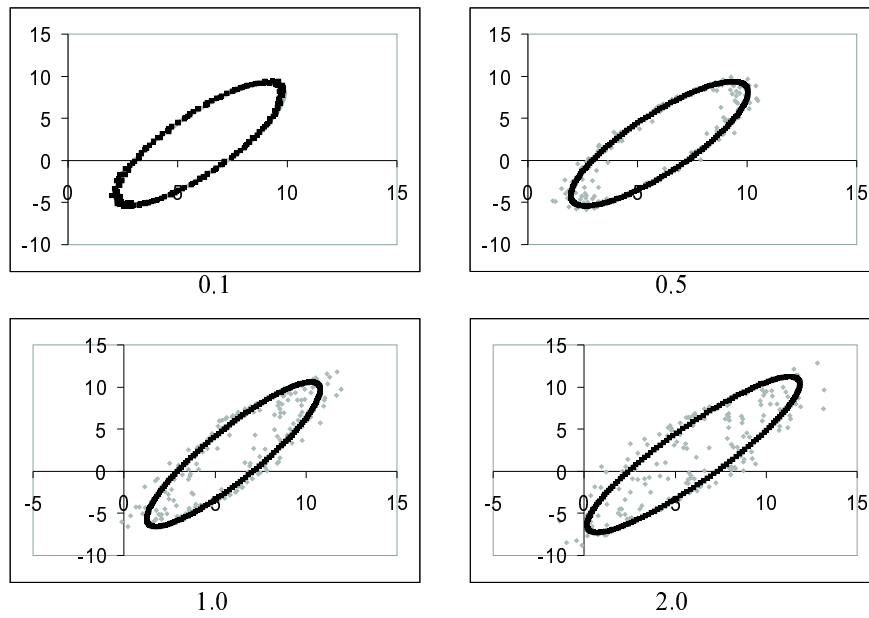
Therefore we set the partial derivatives $\partial D_s / \partial a$, $\partial D_s / \partial b$, $\partial D_s / \partial c$, $\partial D_s / \partial d$ and $\partial D_s / \partial e$ equal to zero. This gives us a system of five linear equations and

five unknowns. To solve this system, the Gauss-Seidel method with successive overrelaxation was used. After the coefficients a , b , c , d and e are determined, the geometrical parameters of the ellipse (position of the center, length of the semi major and the semi minor axes and the orientation of the ellipse) can be calculated by reduction of the quadratic equation. In Figure 4, examples are shown. First, a set of data points with known parameters was generated, then noise was added and finally, the parameters were fitted to the noisy data.

To determine the parameters of the cone, we used the fact that the semi major axes of ellipses in subsequent slices are sides of conformal triangles. This gives us a relation between the semi major axis of an ellipse in a certain slice and the number of the slice in function of the parameters of the cone (opening angle and orientation of the axis of the cone). With least square fitting, these parameters can be calculated.

References

- [1] The restoration of hst images and spectra ii. Proceedings of a Workshop, 1993.
- [2] D. Bird and S. Corbato. *Physical Review Letters*, 71(21).
- [3] J. M. Byrne. A study of cosmic ray nuclei, with charge $Z \geq 2$, at civil aviation altitudes in the earth's atmosphere. Master's thesis, University of Dublin, 1995.
- [4] A. Fitzgibbon, M. Pilu, and R. Fischer. International conference on pattern recognition. In *Proc. of SPIE*, Vienna, Austria, 1996.
- [5] R. L. Fleischer, B. Price, and R. M. Walker. *Nuclear Tracks in Solids*. University of California Press, 1975.
- [6] M. Gu. *Principles of Three-Dimensional Imaging in Confocal Microscopes*. World Scientific Publishing, 1996.
- [7] R. J. e. Hanisch. Restoration newsletter of stsci's image restoration project. Newsletter, 1993.
- [8] P. C. Hansen. Numerical aspects of deconvolution. lecture notes IMM-LEC-1, 1999.
- [9] R. Henke and E. Benton. On geometry of tracks in dielectric nuclear track detectors. *Nuclear Instruments and Methods*, (97), 1971.
- [10] J. W. Lichtman. Confocal microscopy. *Scientific American*, (17), 1994.
- [11] N. C. on Radiation Protection and Measurements. Guidance on radiation received in space activities. Technical Report 98, Fandord University, 1989.
- [12] J. Pláček and J. Reichig. Transmitted-light microscopy for biology: A physicists' point of view part 1. In *Proceedings RMS*, volume 33, 1998.
- [13] W. H. Press, S. A. Teukolsky, and W. T. Vetterling. *Numerical Recipes in C*. Cambridge University Press, 1988, 1992.
- [14] G. Somogyi. Development of etched nuclear tracks. *Nuclear Instruments and Methods*, (173), 1980.
- [15] S. S. Somogyi, G. Track-diameter kinetics in dielectric track detectors. *Nuclear Instruments and Methods*, (109), 1973.
- [16] H. van der Voort and K. Strasters. Restoration of confocal images for quantitative image analysis. *Journal of Microscopy*, 178, 1994.
- [17] H. van der Voort and K. Strasters. A quantitative comparison of image restoration methods for confocal microscopy. *Journal of Microscopy*, 185(3):354–365, 1997.
- [18] G. van Kempen, L. van Vliet, and H. van der Voort. Restoration of confocal images for quantitative image analysis. *Journal of Microscopy*, 178:165–181, May 1995.
- [19] P. Verveer, M. Gemkow, and T. Jovin. A comparison of image restoration approaches applied to three-dimensional confocal and wide-field fluorescence microscopy. *Journal of Microscopy*, 193:50–61, 1999.



		a	b	x_0	y_0
0.0	114.59	8.00	2.00	6.00	2.00
0.1	115.21	8.00	2.01	6.01	1.98
0.5	116.18	8.17	2.03	6.00	1.97
1.0	117.61	9.63	1.91	6.02	2.02
2.0	121.20	10.73	2.14	6.00	1.98

Figure 4: Results from the ellipse fitting algorithm